0026-895X/01/6002-394–402$3.00
MOLECULAR PHARMACOLOGY
Copyright © 2001 The American Society for Pharmacology and Experimental Therapeutics
Mol Pharmacol 60:394–402, 2001

Vol. 60, No. 2
837/921708
Printed in U.S.A.

Histone H3 Phosphorylation Is Coupled to Poly-(ADP-Ribosylation) during Reactive Oxygen Species-Induced Cell Death in Renal Proximal Tubular Epithelial Cells

KULBHUSHAN TIKOO, SERRINE S. LAU, and TERRENCE J. MONKS

Center for Molecular & Cellular Toxicology, Division of Pharmacology and Toxicology, College of Pharmacy, University of Texas at Austin, Austin, Texas

Received January 23, 2001; accepted May 14, 2001

This paper is available online at http://molpharm.aspetjournals.org

ABSTRACT

Although the cellular response to chemical-induced stress is relatively well characterized, particularly the response to DNA damage, factors that govern the outcome of the stress response (cell survival or cell death) are less clearly defined. In this context, the mitogen-activated protein kinase (MAPK) family responds to a variety of physical and chemical stresses. The activation of MAPKs, especially the extracellular-regulated protein kinase subfamily, seems to play a causal role in death of renal proximal tubular epithelial cells (LLC-PK1) induced by reactive oxygen species (ROS). In this study, we show that extracellular signal receptor-activated kinase (ERK) activation may be coupled with LLC-PK1 cell death via changes in chromatin structure, which is mediated by increases in the phosphorylation of histone H3 (a post-translational modification required for both chromosome condensation and segregation during mitosis) and premature chromatin/chromosomal condensation, leading to cell death. In support of this view, 2,3,5-*tris*-(glutathion-*S*-yl)hydroquinone (TGHQ)-induced phosphorylation of histone H3 is accompanied by increases in chromatin condensation, as observed with the use of 4,6-diamidino-2-phenylindole-fluorescent staining, and by decreases in the sensitivity of chromatin to digestion by micrococcal nuclease. Changes in chromatin structure precede cell death. TGHQ-induced histone H3 phosphorylation and chromatin condensation are inhibited by PD098059, which selectively inhibits MAPK kinase, an upstream regulator of ERKs. Moreover, histone phosphorylation is modulated by poly(ADP-)ribosylation. Thus, the inhibition of poly(ADP-ribose)polymerase with 3-aminobenzamide prevents histone H3 phosphorylation and increases cell survival, suggesting that ADP-ribosylation and histone H3 phosphorylation are coupled in this model of ROS-induced DNA damage and cell death. The coupling of histone phosphorylation with ribosylation has not been previously demonstrated.

Mechanisms of cell death are usually classified into two pathways: apoptosis and necrosis. However, it has been proposed that the term *oncosis,* with its root from the Greek meaning "swelling," be used as the alternate descriptor of cell death occurring by nonapoptotic pathways (Trump et al., 1997). The word *necrosis* describes more accurately the consequences of oncotic cell death, usually the death of a large number of cells that results in moderate to severe tissue injury. Accordingly, apoptosis is a genetically controlled process, requiring the coordinated suppression and expression of key genes and is characterized by an orchestrated series of processes that can be separated into two general phases: the "commitment" phase and the "execution" phase. In addition, apoptosis requires energy and usually involves the participation of individual, noncontiguous cells. The morphological features of apoptosis usually include cell shrinkage, chromatin condensation and margination, DNA fragmentation into nucleosomal-sized remnants, membrane blebbing, and the formation of apoptotic bodies. Oncosis is generally considered a passive process, with the cell responding to external stress in an uncoordinated, random fashion, dependent on the nature of the specific stress. Oncosis is a form of cell death that typically occurs in response to toxic injury, including that induced by chemical exposure and reactive oxygen species (ROS). In contrast to apoptosis, oncosis is characterized by cell and organelle swelling that eventually leads to the loss of plasma membrane integrity.

ROS are involved in the initiation and progression of a variety of human diseases (Kehrer, 1993), including renal ischemia/reperfusion injury and in toxicities associated with chemical exposure. An understanding of the factors that regulate the cellular response to ROS and the molecular mechanisms by

This work was supported in part by an award from the National Institute of Environmental Health Sciences (ES07359) to TJM. Portions of this work have been presented in abstract form at the *Keystone Symposium on Chromatin Structure and Function*; 2000 Feb 12–18; Durango, Colorado; Abstract #223, and at the *39th Annual Meeting of the Society of Toxicology*; 2000 Mar 19–23; Philadelphia, Pennsylvania; *Toxicol. Sci*. 2000; **54:**212.

ABBREVIATIONS: ROS, reactive oxygen species; PCC, premature chromatin condensation; ERK, extracellular signal-regulated kinase; TGHQ, 2,3,5-*tris*-(glutathion-*S*-yl)hydroquinone; DAPI, 4,6-diamidino-2-phenylindole; DCFDA, 2,7-dichlorofluorescein diacetate; DMEM, Dulbecco's modified Eagle's medium; LC-MS/MS, liquid chromatography tandem mass spectrometry; amu, atomic mass units; MAPK, mitogen-activated protein kinase; PARP, poly(ADP-ribose)polymerase; MSK1, mitogen- and stress-activated protein kinase.

which they interact with cellular constituents, as well as the consequences of such interactions, are important fundamental goals of biomedical research. Renal proximal tubule epithelial cells are particularly sensitive to oxidant-mediated injury. Using a well-established in vitro model of renal proximal tubule epithelial cells (LLC-PK1), we have shown that treatment of LLC-PK1 cells with quinol-thioethers produces single-strand breaks in DNA, rapid growth arrest, modulation of stress- and growth-gene expression, and cell death (Monks and Lau, 1998).

The signal transduction pathways activated during the commitment phase of oncotic cell death are insufficiently characterized. A pivotal event during the cell cycle is the timing of the initiation of DNA replication (*S*-phase entry). Rigid controls function to prevent repeated rounds of DNA replication without intervening mitoses, as well as to prevent the initiation of mitosis before DNA replication is complete ("mitotic catastrophe"). Although some of the genetic interactions that participate in this process have recently been identified in yeast (Novak and Tyson, 1997), little is known about their mammalian counterparts. A frequent response to ROS-induced cell stress that ultimately leads to oncotic cell death is premature chromatin condensation (PCC) and the ensuing mitotic catastrophe (Novak and Tyson, 1997). Because a variety of phosphatase inhibitors induce PCC (Coco-Martin and Begg, 1997), protein phosphorylation must play an important role in this process. However, the targets for phosphorylation and the corresponding protein kinases are poorly defined. During the transition from the G_2 phase into mitosis, relaxed interphase chromatin must be converted into mitotic condensed chromatin, a process considered essential for nuclear division. However, relatively little is known about the mechanisms and factors that regulate this transition in chromatin structure (Koshland and Strunnikov, 1996).

Phosphorylation of histones H1 and H3 has long been implicated in chromosome condensation during mitosis (Koshland and Strunnikov, 1996). Increases in histone H1 kinase activity during heat shock occur coincidentally with PCC and are associated with M-phase kinase complexes containing cyclin B1 (Mackey et al., 1996). Early studies demonstrated that increases in H1 phosphorylation occurred during mitosis in a variety of eukaryotes (Roth and Allis, 1992). However, although H1 hyperphosphorylation is temporally associated with entry into mitosis and requires Cdc2 kinase activity (Langan et al., 1989), recent studies indicate that chromatin condensation can occur in the absence of this modification (Guo et al., 1995) and even without H1 itself (Shen et al., 1995). In contrast to the data on H1 phosphorylation, experimental evidence strongly implicates a functional role for H3 phosphorylation in chromosome condensation (Wei et al., 1999). The present study was therefore initiated to test the hypothesis that ERK activation in renal epithelial cells is coupled with PCC and cell death via the activation of downstream histone H3 kinase(s).

Materials and Methods

Cell Culture and Treatment Conditions. LLC-PK1 cells (American Type Culture Collection, Manassas, VA), a renal proximal tubule epithelial cell line derived from the New Hampshire mini-pig, were maintained in Dulbecco's modified Eagle's medium (DMEM) containing 10% fetal bovine serum and high glucose without pyruvate (Invitrogen, Carlsbad, CA) at 37°C in a humidified incubator containing 5% CO_2. Cells were seeded at a density of 2×10^6 cells/100-mm dish and were used after overnight culture. Cultures were washed twice with Hanks' balanced salt solution and then treated with TGHQ in DMEM containing 20 mM HEPES.

Fluorescence Microscopy. Cells growing on cover slips treated with TGHQ for 2 h, as well as untreated control cells, were fixed with 3.7% formaldehyde in ice-cold phosphate-buffered saline for 10 min and then treated with methanol at −20°C for 10 min. DNA was stained with 0.5 μg/ml 4′,6-diamidino-2-phenylindole (DAPI) (Roche Molecular Biochemicals, Summerville, NJ) for 10 min at room temperature. Cells were examined with an Olympus BH2-RFCA microscope (Olympus, Tokyo, Japan).

Fluorescence Confocal Microscopy and Fluorescent Probes. A laser fluorescence confocal microscope (Meridian Instruments, Okemos, MI) was used to evaluate the role of TGHQ-induced ROS production using 2,7-dichlorofluorescein diacetate (DCFDA) as the fluorophore. Cleavage of the acetate moiety by esterases traps 2,7-dichlorofluorescein inside the cell, where it is available for oxidation by ROS to yield the fluorescent 2,7-dichlorofluorescein. Excitation was provided by a water-cooled argon ion laser with spectral line at 488 nm. Emission was measured after passing a 575-nm dichroic short-pass filter. The light transmitted through this filter traveled through a 530-nm bandpass filter. LLC-PK1 cells were plated onto 2-well Lab-Tek glass chambers (Nalge Nunc International, Naperville, IL) 2 days before the experiment at a density of 70,000 cells/well. Kinetic analysis of ROS was performed at room temperature in the presence or absence of TGHQ. Cells were loaded with DCFDA (10 μM) for 30 min at 37°C and were scanned in the continued presence of DCFDA. An area of cells was selected and scanned once to determine basal levels of ROS; TGHQ was added, and changes in fluorescence were recorded every 5 min for 25 min.

Chromatin Fractionation after Digestion with Micrococcal Nuclease. After treatment of cells with TGHQ for 1 h in the presence and absence of 3-aminobenzamide or PD098059, nuclei were isolated under low ionic strength buffer conditions (Tikoo et al., 1997). The isolated nuclei were subsequently suspended in "nuclei buffer" (10 mM Tris-HCl, pH 7.4, 10 mM NaCl, and 1 mM phenylmethylsulfonyl fluoride) at a concentration of 1 mg/ml. Nuclei were then digested with micrococcal nuclease (1 unit/mg DNA) at 37°C for 5 min, and the reaction was terminated by adding 10 mM EDTA. The supernatants, containing digested chromatin fragments, were collected by centrifugation of nuclei at 12,000*g* for 10 min, and the absorbance at 260 nm was determined and expressed as a percentage of the total nuclear absorbance (supernatant and pellet).

Metabolic Labeling of Cells and Histone Extraction for Phosphorylation Studies. To determine the effect of TGHQ-induced oxidative stress on histone phosphorylation, LLC-PK1 cells were labeled with 40 μCi/ml [^{32}P] orthophosphoric acid in phosphate-free DMEM with 20 mM HEPES for 2 h. Radioactivity was removed after 2 h, and cells were treated with TGHQ in phosphate-free DMEM containing 20 mM HEPES. Cells were washed in ice-cold low-salt buffer (10 mM Tris-HCl, 10 mM NaCl, and 2.5 mM EDTA, pH 7.4) and then lysed in lysis buffer (low-salt buffer containing 0.25 mM sucrose, and 1% Triton X-100). Nuclei were collected by centrifugation at 1000*g* for 5 min. Histones were extracted with 0.25 M HCl and precipitated in 20% trichloroacetic acid. The precipitate was washed twice: once with 0.25 M HCl containing acetone and

then with acetone only. Proteins (measured in micrograms) were loaded in each lane of a 13.5% SDS polyacrylamide gel. After electrophoresis, the proteins were stained with Coomassie Blue, dried, and then exposed to Kodak XAR film (Eastman Kodak, Rochester, NY). Quantification of autoradiograms was performed using Instant Imager Electronic Autoradiography (Packard, Meriden, CT) wherever necessary. For studying the effect of different inhibitors on TGHQ-induced H3 phosphorylation, metabolically labeled cells were pretreated with inhibitors and then cotreated with TGHQ as described in detail in the appropriate figure legends.

Identification of Core Histones by Liquid Chromatography Tandem Mass Spectrometry (LC-MS/MS). Proteins were separated by SDS-polyacrylamide gel electrophoresis as described above. Gels were stained with 0.1% Coomassie Blue R (in 40% methanol/10% acetic acid) and destained with 50% methanol/5% acetic acid. Proteins of interest were identified by the use of autoradiography and an Instant Imager Electronic Autoradiography system (Packard) and were matched with Coomassie Blue staining. Typically, 300 to 600 μg total cellular lysate protein per lane is sufficient for LC/MS analysis. In-gel tryptic digestion was a modification of the method described by Shevchenko et al. (1996). Protein bands were cut from gels and stored at −80°C in a 5% acetic acid solution. Before digestion, protein bands were further cut into 1-mm pieces and destained for another 2 to 3 h. After destaining, gel slices were dehydrated with acetonitrile, and residual acetonitrile was evaporated in a SpeedVac (Thermo Savant, Holbrook, NY). Gel slices were then reduced with 10 mM dithiothreitol (in 100 mM NH_4HCO_3) at room temperature for 1 h. Residual dithiothreitol was removed, and gel slices were alkylated with 50 mM iodoacetamide and then subjected to washing and dehydration (100 mM NH_4HCO_3, 10 min; twice acetonitrile, 5 min; 100 mM NH_4HCO_3, 10 min; twice acetonitrile, 5 min). Gels were dried for 2 to 3 min in a SpeedVac and rehydrated on ice with 20 ng/μl sequencing grade modified trypsin (in 50 mM NH4HCO3; Promega, Madison, WI) for 10 to 15 min. Excess trypsin was removed, 20 μl of 50 mM NH_4HCO_3 was added, and gel slices were digested overnight at 37°C. After in-gel digestion, peptides were extracted twice in 75 μl of 5% formic acid/50% acetonitrile, evaporated to a volume <25 μl, and subjected to LC-MS/MS analysis. High-performance LC-MS/MS was performed on tryptic digests with a Finnigan-MAT LCQ (Thermo Finnigan, San Jose, CA) electrospray ion-trap mass spectrometer coupled with a MAGIC 2002 microbore high-performance liquid chromatograph (Michrom BioResources, Auburn, CA). Acquisition of MS-MS spectra was carried out by data-dependent scanning with Finnigan Excalibur software (Thermo Finnigan). Total run time was typically 45 min. Peptides were analyzed on a MAGIC MS C18 microbore column (5 μm, 200 A, 0.5 × 50 mm; Michrom BioResources) and washed with mobile phase A [acetonitrile/water/acetic acid/trifluoroacetic acid (2:98:0.1:0.02, v/v)] for 5 min, and then eluted with mobile phase B [acetonitrile/water/acetic acid/trifluoroacetic acid (90:10:0.09:0.02, v/v)] using a linear gradient from 5 to 65% mobile phase B over 30 min, increased to 95% mobile phase B and held for 5 min at a flow rate of 20 μl/min. Data-dependent scanning was performed with a default charge state of 2, an isolation width of 2.0 amu, normalized collision energy of 35%, an activation time of 30.0 ms, and a required minimum signal of 50,000 counts. Global dependent data settings were an exclusion mass width of 1.5 amu, a reject mass width of 1.0 amu with dynamic exclusion enabled, a repeat count of 2, a repeat duration of 1.0 min and an exclusion duration of 1.0 min. The scan event series include one full scan with a mass range of 400 to 2000 Da, followed by one dependent MS-MS scan of the most intense ion. Capillary temperature, sheath gas pressure, and auxiliary gas pressure were set at 200°C, 60 psi, and 0 psi, respectively. Individual peptide sequences were identified with the SEQUEST program incorporated into Finnigan MAT BIOWORKS software (Thermo Finnigan) to translate MS/MS spectra to amino acid sequences in the nonredundant OWL protein database (http://www.bis-.med.jhmi.edu/Dan/proteins/owl.html).

Neutral Red Assay for Cell Viability. Cells were seeded at a density of 1×10^5 cells/well in 24-well plates and were used after 24 h of culture. Cells were washed and treated with TGHQ in DMEM containing HEPES. Viability was then determined with the neutral red assay as described previously (Mertens et al., 1995).

Statistical Analysis. All data are expressed as mean ± S.E.M. Mean values were compared by the use of analysis of variance with a post hoc Student-Newman-Keuls test. $P < 0.05$ was accepted as significant.

Results

Morphological Changes in Cells Undergoing Cell Death. The morphological alterations seen after TGHQ treatment of LLC-PK1 cells were similar to those we described previously after the administration of a structurally and toxicologically similar halogenated analog, 2-Br-*bis*-(glutathion-*S*-yl)hydroquinone (Rivera et al., 1994). The margination of heterochromatin seems random in nature and does not conform to the typical crescent-type margination associated with cells undergoing apoptosis. Consistent with the in vivo observations, DAPI-stained nuclei of cells after treatment with TGHQ also exhibit aggregation and margination of chromatin (Fig. 1C). In contrast, nuclei of untreated control LLC-PK1 cells exhibit a diffuse pattern of DAPI-staining, reflecting the even distribution of chromatin throughout the nuclei (Fig. 1A).

Chromatin Sensitivity to Micrococcal Nuclease. To lend support to the presence of enhanced chromatin condensation in cells undergoing TGHQ-induced cell death, chromatin sensitivity to micrococcal nuclease was determined. Micrococcal nuclease cleaves chromatin preferentially at hypersensitive sites, and decreases in sensitivity to cleavage occur after PCC because the hypersensitive sites are shielded from the enzyme. Nuclei from LLC-PK1 cells treated with TGHQ (0, 50, 100, 200, or 400 μM) for 1 h were isolated under low ionic strength buffer conditions to prevent rearrangement and exchange of histone H1 and higher order folding of chromatin. Chromatin sensitivity to micrococcal nuclease decreased by ~60% in nuclei isolated from LLC-PK1 cells treated with 400 μM TGHQ (Fig. 2) (percentage nuclear absorbance at 260 nm in supernatant of control and TGHQ-treated cells = 25.7 ± 1.16% and 10.6 ± 0.46%, respectively). This finding confirms the view that chromatin within these cells is in a more condensed state than that in untreated control cells.

Identification of Histones by LC-MS/MS. To confirm both the identity and purity of the putative histone H3 gel band, LC-MS/MS was performed on in-gel tryptic digests of the excised protein. The following peptides were identified: DIQLAR, EIAQDFK, YRPGTVALR, and STELLIR, providing a coverage of 21.5% and definitive evidence that the

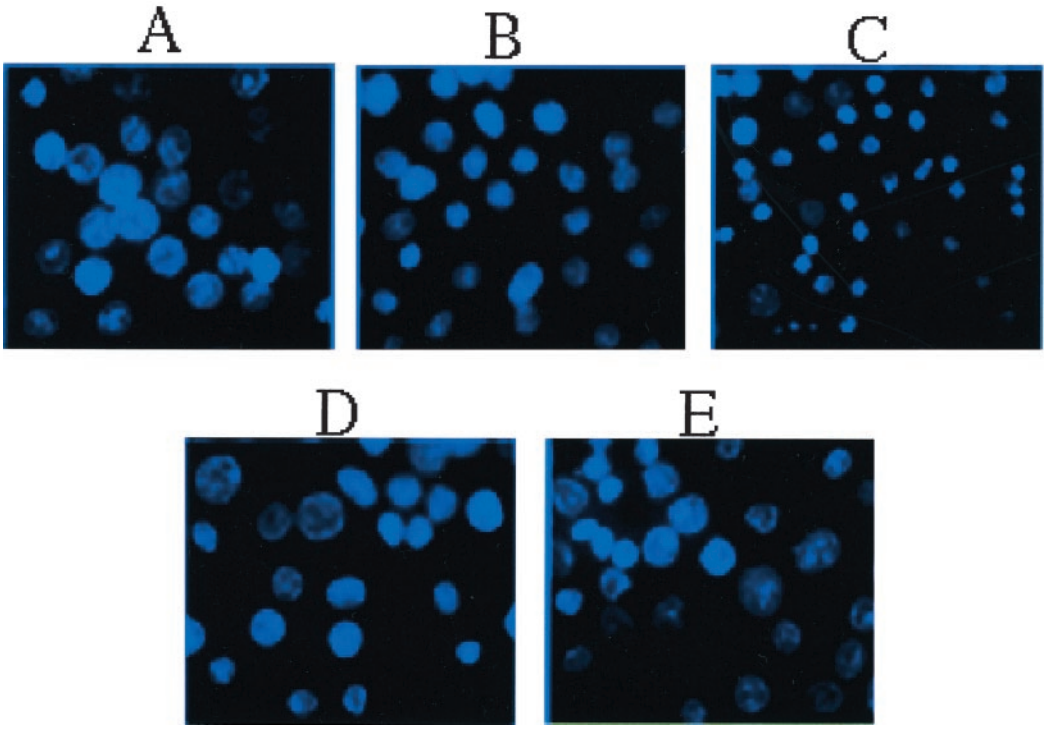

Fig. 1. TGHQ-induced chromatin condensation in LLC-PK1 cells. LLC-PK1 cells were cultured at 2×10^4/ml density overnight and then treated with 400 μM TGHQ for 2 h in the presence and absence of pharmacological inhibitors. LLC-PK1 cells were washed with phosphate-buffered saline and stained with DAPI as described under *Materials and Methods*. DAPI-stained cells were observed under a fluorescent microscope. Control untreated cells (A), TGHQ-treated for 1 h (B), for 2 h (C), for 2 h in the presence of 3-aminobenzamide (1 mM) (D), or PD 98059 (50 μM) (E).

digested protein was indeed histone H3. No contaminating peptides were observed on LC-MS/MS analysis. Similar analyses were performed on the gel bands representative of the core histones. The histone H2B gel band yielded two peptides, KESYSVYVYK and LLLPGELAK, providing 21.6% coverage; histone H2A yielded five peptides, NDEELNK, IIPR, HLQLAIRNDEELNK, AGLQFPVGR, and VTIAQGGVLPNIQ AVLLPK, providing 35.7% coverage; and histone H4 yielded six peptides, DNIQGITKPAIR, ISGLIYEETR, VFLENVIR, KTVTAMDVVYALK, TVTAMDVVYALKR, and TVTAMDVVYALK, providing 43.1% coverage.

Histone Phosphorylation in Response to TGHQ-Induced Oxidative Stress. Phosphorylation of histone H3 is required for chromosome condensation and segregation in vivo (Wei et al., 1999) and also occurs during PCC (Hanks et al., 1983). Inappropriate histone H3 phosphorylation might therefore initiate chromosomal condensation, and premature

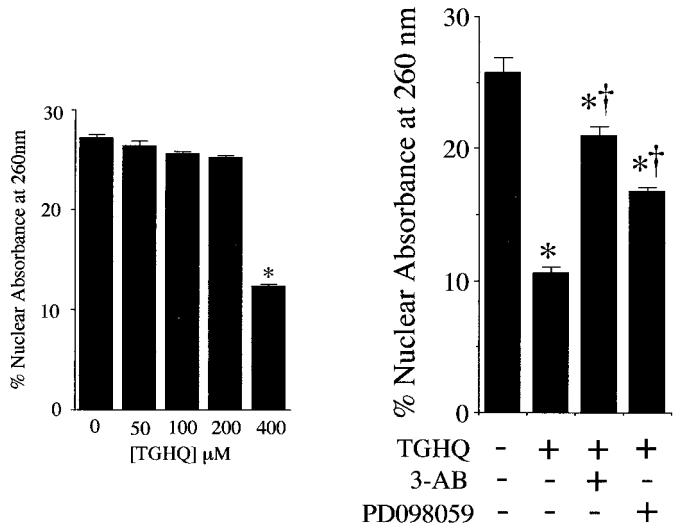

Fig. 2. Decreases in micrococcal nuclease sensitivity reflect TGHQ-induced chromatin condensation in LLC-PK1 cells. Left, nuclei isolated from LLC-PK1 cells treated with 0, 50, 100, 200, or 400 μM TGHQ. Right, nuclei isolated from control LLC-PK1 cells or cells treated with 400 μM TGHQ for 1 h in the absence or presence of 3-aminobenzamide or PD98059. The data represent the percentage of the nuclear absorbance of the supernatant from micrococcal nuclease (1 unit/mg DNA)-digested chromatin. Absorbance at 260 nm is determined and expressed as a percentage of the total nuclear absorbance. The data represent the mean ± S.E.M. for two separate experiments, with each experiment carried out in triplicate. *Significantly difficult from controls at $p < 0.01$. †Significantly different from TGHQ-treated cells at $p < 0.01$.

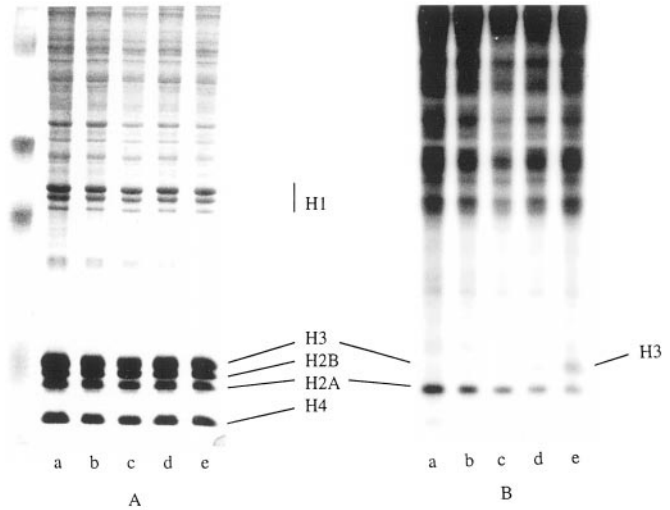

Fig. 3. TGHQ induces histone H3 phosphorylation and histone H2A dephosphorylation in LLC-PK1 cells. LLC-PPK1 cells were labeled with 40 μCi/ml [^{32}P]orthophosphoric acid for 2 h and then treated with increasing concentrations of TGHQ for 30 min. Histones were extracted from these cells and 40 μg protein was electrophoretically resolved on a 13.5% SDS-polyacrylamide gel as described under *Materials and Methods*. Lane a, untreated control cells. Lane b, 50 μM TGHQ; lane c, 100 μM TGHQ; lane d, 200 μM TGHQ; lane e, 400 μM TGHQ. A, Coomassie Blue-stained gel. B, corresponding autoradiograph.

entry into mitosis might lead to mitotic catastrophe and cell death. We therefore determined the effects of TGHQ-generated ROS on histone phosphorylation in LLC-PK1 cells. Treatment of LLC-PK1 cells with TGHQ (50–400 μM) (Fig. 3) induces changes in histone phosphorylation within 30 min of exposure. In particular, TGHQ-induced oxidative stress is accompanied by dephosphorylation of histone H2A, followed by the subsequent phosphorylation of histone H3 (Fig. 3). Phosphorylation of histone H3 occurs at concentrations of TGHQ that commit LLC-PK1 cells to oncotic cell death via premature chromatin condensation (Fig. 3, lane e). Thus, phosphorylation of histone H3 occurs rapidly after exposure of cells to TGHQ and accompanies decreases in neutral red absorption (Fig. 4C). Because neutral red is a measure of lysosomal integrity and precedes cell death measured by loss of plasma membrane integrity by 60 to 90 min (Mertens et al., 1995), phosphorylation of histone H3 precedes cell death (Fig. 4). Although TGHQ also seems to increase the phosphorylation of histone H4 (Fig. 4B), only the phosphorylation of histones H1 and H3 are presently known to modulate chromatin structure (Wolffe, 1995). It should also be noted that the time-dependent increase in histone H2A phosphorylation in TGHQ-treated cells (Fig. 4) is considerably lower than that observed in control cells over time, because histone H2A phosphorylation occurs throughout the cell cycle (Wolffe, 1995).

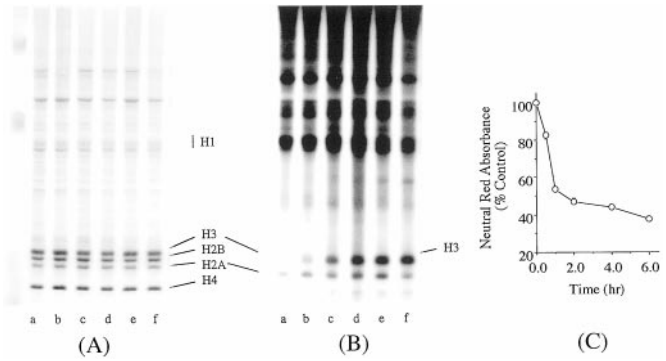

Fig. 4. Changes in histone phosphorylation precede cell death in TGHQ-treated LLC-PK1 cells. [^{32}P]Orthophosphoric acid-labeled LLC-PK1 cells were treated with 400 μM TGHQ for increasing periods of time. Histones were extracted from these cells and 25 μg of protein was electrophoretically resolved on a 13.5% SDS polyacrylamide gel as described under *Materials and Methods.* Lane a, untreated control cells; lane b, 15 min; lane c, 30 min; lane d, 60 min; lane e, 120 min; lane f, 180 min. A, Coomassie Blue-stained gel. B, the corresponding autoradiograph. C, cell viability was determined using the neutral red assay as described under *Materials and Methods.*

TGHQ-induced DNA damage, growth arrest, stress- and growth-related gene expression, and cell death are all dependent on the generation of ROS (Monks and Lau, 1998). Consistent with these findings, TGHQ increases the oxidation of 2,7-dichlorodihydrofluoroscein to the green fluorescent 2,7-dichlorofluoroscein (Fig. 5). We subsequently determined the effects of catalase on TGHQ-induced histone H3 phosphorylation. Consistent with previous findings regarding the requirement for ROS in TGHQ-induced cell death, catalase (10 units/ml) prevented histone H3 phosphorylation (Fig. 6).

PD98059, a Selective MAPK Kinase Inhibitor, Inhibits TGHQ-Induced Histone H3 Phosphorylation. Histone H3 is phosphorylated rapidly in response to growth factors, phorbol esters, okadaic acid, and protein synthesis inhibitors (Mahadevan et al., 1991). Recent studies have shown that phorbol ester-induced histone H3 phosphorylation requires ERK activation and is blocked by PD98059 (Wei et al., 1999). We have shown recently that TGHQ induces ERK activation in LLC-PK1 cells and that inhibition of ERK correlates with increases in cell survival. (Q. Huang, S. S. Law, and T. J. Monks, unpublished observations). TGHQ-induced H3 phosphorylation is also blocked (~90%) by pretreatment of LLC-PK1 cells with PD98059 (50 μM) (Fig. 7), a selective inhibitor of mitogen-activated protein kinase kinase, which is an upstream regulator of ERK activity. The changes in histone H3 phosphorylation are accompanied by decreases in both chromatin condensation (Fig. 1E) and in chromatin sensitivity to micrococcal nuclease digestion (Fig. 2B). Collectively, the data indicate that the nuclear response to TGHQ is coupled with ERK activation. TGHQ-generated ROS probably initiate a cascade of events that leads to cell death; histone H3 phosphorylation is a major component of this cascade, which causes changes in chromatin structure.

Modulation of Histone Phosphorylation by Poly-ADP Ribosylation. DNA strand breaks caused by ROS lead to the activation of poly(ADP-ribose)polymerase (PARP), the excessive activation of which results in the depletion of both NAD^+ and ATP (Pieper et al., 1999). It has been suggested that depletions in NAD and ATP in response to DNA damage contribute to cell death as a consequence of deficits in energy stores. Consistent with this view, inhibitors of PARP protect

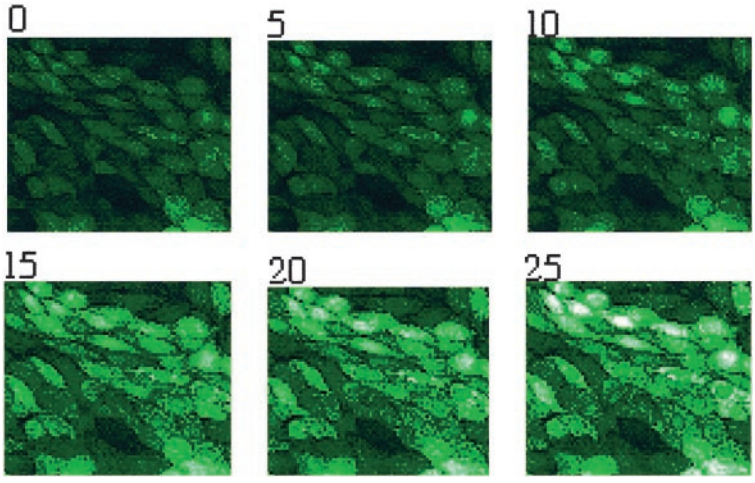

Fig. 5. TGHQ-induced ROS generation in LLC-PK1 cells. LLC-PK1 cells were plated onto 2-well Lab-Tek glass chambers 2 days before the experiment at a density of 70,000 cells/well. Analysis of ROS was performed at room temperature in the presence or absence of TGHQ (200 μM). Cells were loaded with DCFDA (10 μM) for 30 min at 37°C and scanned in the continued presence of DCFDA. An area of cells was selected and scanned once to determine basal levels of ROS, then no addition (for control) or different concentrations of TGHQ (for experimental treatment) was added, and changes in fluorescence were recorded every 5 min for 25 min.

against H_2O_2-mediated cell death (Cristovao and Rueff, 1996). In particular, PARP is activated in LLC-PK1 cells exposed to H_2O_2, and pretreatment of cells with 3-aminobenzamide completely prevents H_2O_2-induced increases in PARP activity (Filipovic et al., 1999) and cell death (Chatterjee et al., 1999). We subsequently investigated the role of PARP in TGHQ-induced cell death and histone H3 phosphorylation. Pretreatment of LLC-PK1 cells with 3-aminobenzamide (1 mM) for 30 min substantially decreased histone H3 phosphorylation (Fig. 8) under conditions suggesting that 3-aminobenzamide increases global protein phosphorylation (Fig. 8). In particular, inhibition of ADP-ribosylation seems to significantly enhance histone H2A phosphorylation, and 3-aminobenzamide overrides TGHQ-mediated decreases in histone H2A phosphorylation (Fig. 8, lane d). Concomitant with the inhibition of TGHQ-induced histone H3 phosphorylation, 3-aminobenzamide also decreased chromatin condensation as evidenced by DAPI staining (Fig. 1D), decreased chromatin sensitivity to micrococcal nuclease digestion (~70%; Fig. 2B), and increased cell viability (Fig. 8C). The data are indicative of a causal relationship between the inhibition of PARP activity and histone H3 phosphorylation. The TGHQ-induced nucleosomal response was not prevented by aurintricarboxylic acid or zinc (data not shown), both of which are inhibitors of endonucleases and proteases (Stennicke and Salvesen, 1997), suggesting that histone H3 phosphorylation is independent of endonuclease or protease activation in this model of ROS-induced cell death.

Discussion

We provide evidence that ROS-induced oncotic cell death of renal proximal tubular epithelial cells involves changes in chromatin structure that are dependent on the phosphorylation of histone H3. Thus, fluorescent labeling of TGHQ-treated LLC-PK1 cells with DAPI revealed the presence of aggregated and condensed chromatin (Fig. 1). The decreased susceptibility of chromatin isolated from TGHQ-treated cells to micrococcal nuclease provides biochemical confirmation of the immunohistochemical findings. Moreover, the biochemical and immunohistochemical findings in LLC-PK1 cells are consistent with changes in chromatin structure that occur in vivo in renal proximal tubular epithelial cell nuclei after exposure of rats to a structurally related quinol-thioether (Rivera et al., 1994). It is possible that direct adduction of TGHQ to chromatin leads to disruption of nucleosomal integrity, although we consider this unlikely. Thus, ROS play a major role in disrupting nuclear architecture because catalase protects against histone H3 phosphorylation (Fig. 6). Catalase would not be expected to have an effect on the adduction of proteins by TGHQ-derived reactive electrophilic metabolites. The mechanism(s) underlying the changes in chromatin structure seem to include the ERK-regulated phosphorylation of histone H3 (Figs. 7 and 9).

Phosphorylation of histone H3 is required for chromosome condensation and segregation during mitosis (Wei et al., 1999) and accompanies PCC (Johnson and Rao, 1970; Hanks et al., 1983). Temperature-sensitive mutants of baby hamster kidney cells (tsBN2 cells) (Kai et al., 1983) sustain histone H1 and H3 phosphorylation at temperatures that also induce PCC (Ajiro et al., 1983). However, prevention of PCC occurs concomitant with decreases in H3 phosphorylation and not with H1 phosphorylation (Ajiro and Nishimoto, 1985). Our data therefore suggest that in response to TGHQ-induced oxidative stress, LLC-PK1 cells attempt to engage mitosis by initiating chromosome condensation prematurely. Mitotic histone H3 phosphorylation can occur at Ser-10 and Ser-28 in the amino-terminal tail (Wei et al., 1999) and promotes the disassociation of the histone H3 amino-terminal tail from DNA (Sauve et al., 1999). This change in chromatin structure permits the association of additional factors with DNA. ROS-induced phosphorylation of histone H3

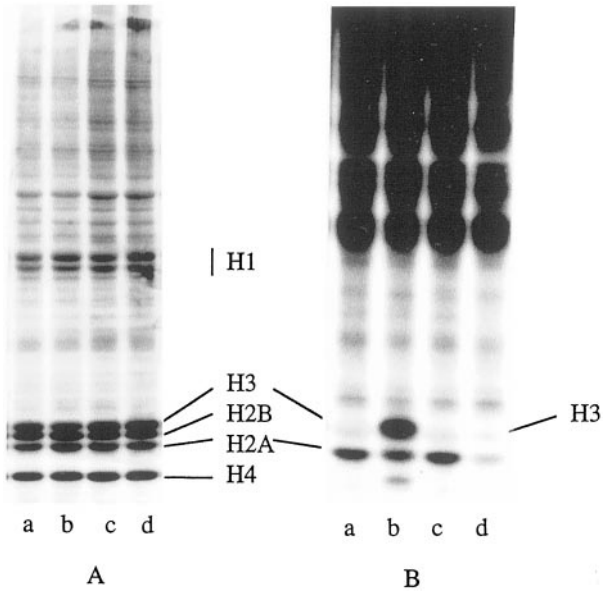

Fig. 6. TGHQ-induced histone H3 phosphorylation in LLC-PK1 cells is dependent on the presence of reactive oxygen species. [^{32}P]Orthophosphoric acid-labeled LLC-PK1 cells were treated for 1 h with 400 μM TGHQ in the presence and in absence of 10 units/ml catalase. Histones were extracted from these cells and 30 μg of protein was electrophoretically resolved on a 13.5% SDS-polyacrylamide gel as described under *Materials and Methods*. Lane a, untreated control cells; lane b, TGHQ-treated cells; lane c, catalase-treated cells; lane d, cells cotreated with TGHQ and catalase. A, Coomassie Blue-stained gel. B, the corresponding autoradiograph.

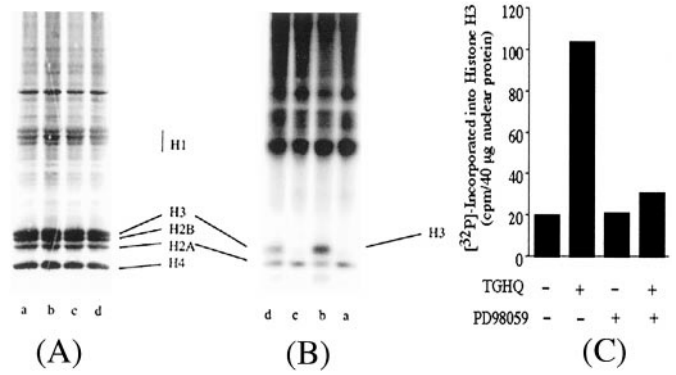

Fig. 7. TGHQ-induced histone H3 phosphorylation is coupled with ERK activation in LLC-PK1 cells. [^{32}P]Orthophosphoric acid-labeled LLC-PK1 cells were pretreated with PD98059 (50 μM) for 30 min and then cotreated with TGHQ (400 μM) for an additional 1 h. Histones were extracted from these cells and 40 μg of protein was electrophoretically resolved on a 13.5% SDS-polyacrylamide gel as described under *Materials and Methods*. Lane a, untreated control cells; lane b, TGHQ-treated cells; lane c, PD98059-treated cells; lane d, cells treated with both PD98059 and TGHQ. A, Coomassie Blue-stained gel. B, the corresponding autoradiograph. C, quantitation (cpm) of [^{32}P] incorporation into histone H3. Quantitation was achieved using a Packard Electronic Instant Imaging system (Packard).

in LLC-PK1 cells might thus result in the exposure of DNA to chromosome-condensing factors, facilitating chromatin condensation.

The mechanisms coupling TGHQ-generated ROS with histone H3 phosphorylation are unclear. H3 phosphorylation, specifically on serine-10, correlates with the induction of immediate-early gene expression. Thus, in mitogen-stimulated mouse fibroblasts, c-fos and c-myc are induced rapidly with concurrent increases in Ser-10 histone H3 phosphorylation (Chadee et al., 1999), thereby linking the MAPK signaling pathway to changes in chromatin structure. We have recently observed the ROS-dependent activation of ERKs after treatment of LLC-PK1 cells with TGHQ and that such activation contributes to oncotic cell death (Q. Huang, S. S. Lau, and T. J. Monks, unpublished observations). These findings provide a possible link between ROS generation and alterations in chromatin structure (Fig. 9). It is likely that one or more kinases downstream of ERK catalyze the phosphorylation of histone H3, triggering PCC and cell death. In support of this view, 1) TGHQ activates ERK1/2 (Q. Huang, S. S. Lau, and T. J. Monks, unpublished observations), 2) TGHQ induces H3 phosphorylation (Figs. 3 and 4), 3) TGHQ-mediated oncotic cell death is inhibited by PD098059 (Q. Huang, S. S. Lau, and T. J. Monks, unpublished observations), and 4) inhibition of ERK1/2 prevents histone H3 phosphorylation (Fig. 7). Several kinases have been implicated as potential histone H3 kinases. In particular, evidence that the nuclear kinase MSK1 has H3 kinase activity provides a potential link completing the circuit between cell surface-sensed stress and nucleosomes (Thomson et al., 1999). MSK1 is activated by both ERKs and the p38 MAPKs (Deak et al., 1998). In addition to MSK1, pp90 ribosomal S6 kinase-2 is required for epidermal growth factor-stimulated phosphorylation of histone H3 in vivo (Sassone-Corsi et al., 1999).

It is well established that PARP activation occurs in response to oxidant-induced DNA strand scission (Masutani et al., 1995). The excessive activation of PARP in response to DNA damage may actually contribute to cell death as a consequence of depletions in both NAD^+ and ATP (Ha and Snyder, 1999). For example, incubation of primary cultures of rat proximal tubule epithelial cells with 1 mM H_2O_2 inhibits mitochondrial respiration and increases lactate dehydrogenase release, with concomitant increases in PARP activity. Inhibitors of PARP protect against H_2O_2-mediated cell death (Chatterjee et al., 1999). In LLC-PK1 cells, 0.5 mM H_2O_2 depletes ATP and causes DNA damage, lipid peroxidation, and oncotic cell death (Andreoli and Mallett, 1997). However, inhibiting lipid peroxidation with lazeroids or Trolox (Hoffman-La Roche, Nutley, NJ) decreased oncotic cell death without affecting DNA damage or depletions in ATP. Thus, DNA damage-induced depletions in cellular ATP concentrations can be dissociated from oncotic cell death. Subsequently, inhibition of PARP was shown to prevent H_2O_2-induced oncosis (1 mM for 2 h) but not apoptosis of LLC-PK1 cells (Filipovic et al., 1999). Thus, 3-aminobenzamide prevented H_2O_2-mediated activation of PARP, restored NAD^+ and ATP concentrations, and prevented early oncotic cell death. However, these cells still subsequently succumb to apoptotic cell death. Inhibition of PARP also shifts the mode of cell death from oncosis to apoptosis in oxidant-stressed endothelial cells (Walisser and Thies, 1999). Using fibroblasts obtained from mice with a targeted deletion of PARP ($PARP^{-/-}$) DNA damage induced by either *N*-methyl-*N*′-nitro-*N*-nitrosoguanidine or H_2O_2 failed to deplete intracellular concentrations of ATP, and the cells were protected against oncotic cell death (Ha and Snyder, 1999) despite exhibiting extensive DNA damage. However, the $PARP^{-/-}$ cells still underwent apoptotic cell death. In contrast, $PARP^{+/+}$ cells treated with either *N*-methyl-*N*′-nitro-*N*-nitrosoguanidine or H_2O_2 died by oncosis, suggesting that PARP activation may regulate the mode of cell death, perhaps by modulating ATP (and possibly NAD^+) concentrations.

Although the biological functions of PARP are unclear, post-translational modification of several nuclear proteins by PARP, including histones, has been implicated in chromatin structure and function, surveillance of the genome, and regulation of proteins that participate in DNA repair (D'Amours et al., 1999). However, under conditions in which PARP is

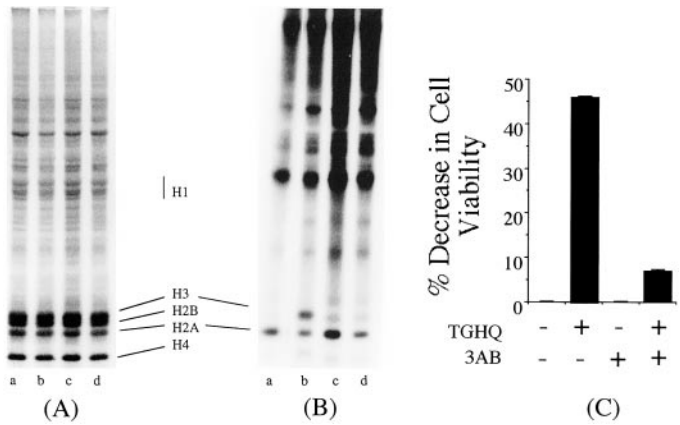

Fig. 8. TGHQ-induced histone H3 phosphorylation and cell death are modulated by PARP activity. Metabolically labeled LLC-PK1 cells were treated for 1 h with 400 μM TGHQ in the presence and absence of 1 mM 3-aminobenzamide. Histones were extracted from these cells and 35 μg of protein was electrophoretically resolved on a 13.5% SDS-polyacrylamide gel as described under *Materials and Methods*. Lane a, untreated control cells; lane b, TGHQ-treated cells; lane c, 3-aminobenzamide-treated cells; lane d, cells pretreated with 3-aminobenzamide and then cotreated with TGHQ. A, Coomassie Blue-stained gel. B, the corresponding autoradiograph. C, cell viability was determined using the neutral red assay as described under *Materials and Methods*.

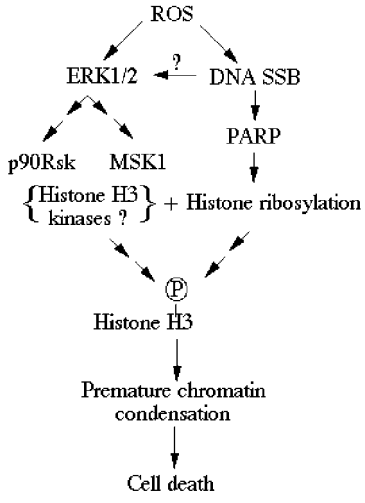

Fig. 9. Proposed pathway coupling ROS generation to alterations in chromatin structure and cell death.

either inhibited pharmacologically or deleted genetically, the potential consequences on PARP targets, as well as their corresponding influence on cell survival, have not been considered. As noted above, DNA damage-induced depletions in cellular ATP concentrations can be dissociated from oncotic cell death. Decreased PARP activity might therefore be cytoprotective against oncotic cell death by interfering with its ability to regulate chromatin structure. PARP participates in histone shuttling and nucleosomal unfolding (Realini and Althaus, 1992) and may facilitate core histone H3 phosphorylation. Consistent with this view, the inhibition of PARP might protect against ROS-induced cell death by modulating ROS-induced histone H3 phosphorylation. Indeed, histone H3 phosphorylation was prevented by 3-aminobenzamide (Fig. 8) at concentrations that produce few other effects (D'Amours et al., 1999), confirming the coupling of ADP-ribosylation and histone H3 phosphorylation (Fig. 9). There is precedence for the coupling of various histone post-translational modifications. For example, Imai et al. (2000) recently described a NAD-dependent histone deacetylase, Sir2, and Sir2 proteins exhibit NAD-dependent mono-ADP-ribosyltransferase activity (Frye, 1999). The coordination of multiple histone modifications seems to be involved in the regulation of immediate-early gene expression (Clayton et al., 2000). In particular, the coupling of histone H3 phosphorylation and acetylation seems to play an important role in transcriptional regulation, particularly in response to factors that engage the epidermal growth factor /MAPK signaling pathway (Clayton et al., 2000).

TGHQ-induced changes in chromatin structure are preceded by the phosphorylation of histone H3 and by the dephosphorylation of H2A (Figs. 3 and 4). Growth factors and phorbol esters induce cell proliferation via the up-regulation of protein kinase C, one of the targets of which are the nuclear histones (Wolffe, 1995). In particular, phosphorylation of histone H2A occurs throughout the cell cycle (Wolffe, 1995), and dephosphorylation of histone H2A should therefore be associated with exit from the cell cycle or cell cycle arrest. Consistent with this view, TGHQ induces a rapid growth arrest in LLC-PK1 cells that is accompanied by the activation of the growth arrest and DNA damage-inducible *gadd153* gene and the down-regulation of histone gene expression (Monks and Lau, 1998). The complete loss of histone H2A phosphorylation has been reported in liver nuclei isolated from growth-arrested hypothyroid rats (Tikoo and Ali, 1997). In addition, because nuclear lamins associate specifically with histones H2A and H2B (Goldberg et al., 1999), it is possible that dephosphorylation of histone H2A within transcriptionally active chromatin may disrupt this interaction with the nuclear matrix, further contributing to chromatin condensation.

Understanding the mechanisms contributing to oncotic cell death has potentially profound clinical implications. The ability to switch the mode of cell death from oncosis to apoptosis will limit secondary inflammation and subsequent cell and tissue damage. For example, in many clinical situations, such as inflammation, vascular stroke, and myocardial infarction, the predominant mechanism of cell death seems to be oncosis. Deletion of PARP protects against *N*-methyl-D-aspartate receptor-activated neurotoxicity (Eliasson et al., 1997), myocardial ischemia (Zingarelli et al., 1998), inflammation elicited by a variety of mediators (Oliver et al., 1999), and streptozocin-induced diabetes (Masutani et al., 1999). In all these models of cell death, the experimental evidence indicates that cell death occurs by oncosis. By extension, it has been predicted that PARP inhibitors may have therapeutic benefit (Ha and Snyder, 1999). Understanding the cellular and molecular mechanisms by which PARP regulates oncotic cell death may therefore lead to additional therapeutic strategies.

Acknowledgments

We thank Dr. Stony Lo and the Analytical Instrumentation Facility Core within the Center for Research in Environmental Disease (ES 07784) for providing the mass spectral analysis of the histones. In addition, we acknowledge the assistance of Rola Barhoumi and Robert C. Burghardt in the Department. of Veterinary Anatomy and Public Health and Image Analysis Laboratory, College of Veterinary Medicine, Texas A&M University, for their assistance with the confocal microscopy.

References

Ajiro K and Nishimoto T (1985) Specific site of histone H3 phosphorylation related to the maintenance of premature chromosome condensation. Evidence for catalytically induced interchange of the subunits. *J Biol Chem* **26:**15379–15381.

Ajiro K, Nishimoto T and Takahashi T (1983) Histone H1 and H3 phosphorylation during premature chromosome condensation in a temperature-sensitive mutant (tsBN2) of baby hamster kidney cells. *J Biol Chem* **258:**4534–4538.

Andreoli SP and Mallett CP (1997) Disassociation of oxidant-induced ATP depletion and DNA damage from early cytotoxicity in LLC-PK1 cells. *Am J Physiol* **272:** F729–F735.

Chadee DN, Hendzel MJ, Tylipski CP, Allis CD, Bazett-Jones DP, Wright JA and Davie JR (1999) Increased Ser-10 phosphorylation of histone H3 in mitogen-stimulated and oncogene-transformed mouse fibroblasts. *J Biol Chem* **274:**24914–24920.

Chatterjee PK, Cuzzocrea S and Thiemermann C (1999) Tempol, a membrane-permeable radical scavenger, reduces oxidant stress-mediated renal dysfunction and injury in the rat. *Kidney Int* **56:**973–984.

Clayton AL, Rose S, Barratt MJ and Mahadevan LC (2000) Phosphoacetylation of histone H3 on c-fos- and c-jun-associated nucleosomes upon gene activation. *EMBO J* **19:**3714–3726.

Coco-Martin JM and Begg AC (1997) Detection of radiation-induced chromosome aberrations using fluorescence in situ hybridization in drug-induced premature chromosome condensations of tumour cell lines with different radiosensitivities. *Int J Radiat Biol* **71:**265–273.

Cristovao L and Rueff J (1996) Effect of a poly(ADP-ribose) polymerase inhibitor on DNA breakage and cytotoxicity induced by hydrogen peroxide and gamma-radiation. *Teratog Carcinog Mutagen* **16:**219–227.

D'Amours D, Desnoyers S, D'Silva I and Poirier GG (1999) Poly(ADP-ribosyl)ation reactions in the regulation of nuclear functions. *Biochem J* **342:**249–268.

Deak M, Clifton AD, Lucocq JM and Alessi DR (1998) Mitogen- and stress-activated protein kinase-1 (MSK1) is directly activated by MAPK and SAPK2/p38, and may mediate activation of CREB. *EMBO J* **17:**4426–4441.

Eliasson MJ, Sampei K, Mandir AS, Hurn PD, Traystman RJ, Bao J, Pieper A, Wang ZQ, Dawson TM, Snyder SH, et al. (1997) Poly(ADP-ribose) polymerase gene disruption renders mice resistant to cerebral ischemia. *Nat Med* **3:**1089–1095.

Filipovic DM, Meng X and Reeves WB (1999) Inhibition of PARP prevents oxidant-induced necrosis but not apoptosis in LLC-PK1 cells. *Am J Physiol* **277:**F428–F436.

Frye RA (1999) Characterization of five human cDNAs with homology to the yeast SIR2 gene: Sir2-like proteins (sirtuins) metabolize NAD and may have protein ADP-ribosyltransferase activity. *Biochem Biophys Res Commun* **260:**273–279.

Goldberg M, Harel A, Brandeis M, Rechsteiner T, Richmond TJ, Weiss AM and Gruenbaum Y (1999) The tail domain of lamin Dm0 binds histones H2A and H2B. *Proc Natl Acad Sci USA* **96:**2852–2857.

Guo XW, Th'ng JPH, Swank RA, Anderson HJ, Tudan C, Bradbury EM and Roberge M (1995) Chromosome condensation induced by fostriecin does not require p34cdc2 kinase activity and histone H1 hyperphosphorylation, but is associated with enhanced histone H2A and H3 phosphorylation. *EMBO J* **14:**976–985.

Ha HC and Snyder SH (1999) Poly(ADP-ribose) polymerase is a mediator of necrotic cell death by ATP depletion. *Proc Natl Acad Sci USA* **96:**13978–13982.

Hanks SK, Rodriguez LV and Rao PN (1983) Relationship between histone phosphorylation and premature chromosome condensation. *Exp Cell Res* **148:**293–302.

Imai S, Armstrong CM, Kaeberlein M and Guarente L (2000) Transcriptional silencing and longevity protein Sir2 is an NAD-dependent histone deacetylase. *Nature (Lond)* **403:**795–800.

Johnson RT and Rao PN (1970) Mammalian cell fusion: induction of premature chromosome condensation in interphase nuclei. *Nature (Lond)* **226:**717–722.

Kai R, Sekiguchi T, Yamashita K, Sekiguchi M and Nishimoto T (1983) Transformation of temperature-sensitive growth mutant of BHK21 cell line to wild-type phenotype with hamster and mouse DNA. *Somatic Cell Genet* **9:**673–680.

Kehrer JP (1993) Free radicals as mediators of tissue injury and disease. *Crit Rev Toxicol* **23:**21–48.

Koshland D and Strunnikov A (1996) Mitotic chromosome condensation. *Ann Rev Cell Biol* **12:**305–333.
Langan TA, Gautier J, Lohka M, Hollingsworth R, Moreno S, Nurse P, Maller J and Sclafani RA (1989) Mammalian growth-associated H1 histone kinase: a homolog of cdc2+/CDC28 protein kinases controlling mitotic entry in yeast and frog cells. *Mol Cell Biol* **9:**3860–3868.
Mackey MA, Zhang XF, Hunt CR, Sullivan SJ, Blum J, Laszlo A and Roti JL (1996) Uncoupling of M-phase kinase activation from the completion of S-phase by heat shock. *Cancer Res* **56:**1770–1774.
Mahadevan LC, Willis AC and Barrah MJ (1991) Rapid histone H3 phosphorylation in response to growth factors, phorbol esters, okadaic acid, and protein synthesis inhibitors. *Cell* **65:**775–783.
Masutani M, Nozaki T, Wakabayashi K and Sugimura T (1995) Role of poly(ADP-ribose) polymerase in cell-cycle checkpoint mechanisms following gamma-irradiation. *Biochimie (Paris)* **77:**462–465.
Masutani M, Suziki H, Kamada N, Watanabe M, Ueda O, Nozaki T, Jishage K, Watanabe T, Sugimoto T, Nakagama H, et al. (1999) Poly(ADP-ribose) polymerase gene disruption conferred mice resistant to streptozotocin-induced diabetes. *Proc Natl Acad Sci USA* **96:**2301–2304.
Mertens JJ, Gibson NW, Lau SS and Monks TJ (1995) Reactive oxygen species and DNA damage in 2-bromo-(glutathion-S-yl) hydroquinone-mediated cytotoxicity. *Arch Biochem Biophys* **320:**51–58.
Monks TJ and Lau SS (1998) The pharmacology and toxicology of polyphenolic-glutathione conjugates. *Annu Rev Pharmacol Toxicol* **38:**229–255.
Novak B and Tyson JJ (1997) Modeling the control of DNA replication in fission yeast. *Proc Natl Acad Sci USA* **94:**9147–9152.
Oliver FJ, Menissier-de Murcia J, Nacci C, Decker P, Andriantsitohaina R, Muller S, de la Rubia G, Stoclet JC and de Murcia G (1999) Resistance to endotoxic shock as a consequence of defective NF-kappaB activation in poly (ADP-ribose) polymerase-1 deficient mice. *EMBO J* **18:**4446–4454.
Pieper AA, Verma A, Zhang J and Snyder SH (1999) Poly (ADP-ribose) polymerase, nitric oxide and cell death. *Trends Pharmacol Sci* **20:**171–181.
Realini CA and Althaus FR (1992) Histone shuttling by poly(ADP-ribosylation). *J Biol Chem* **267:**18858–18865.
Rivera MI, Jones TW, Lau SS and Monks TJ (1994) Early morphological and biochemical changes during 2-Br-(diglutathion-S-yl)hydroquinone-induced nephrotoxicity. *Toxicol Appl Pharmacol* **128:**239–250.
Roth SY and Allis CD (1992) Chromatin condensation: does histone H1 dephosphorylation play a role? *Trends Biochem Sci* **17:**93–98.
Sassone-Corsi P, Mizzen CA, Cheung P, Crosio C, Monaco L, Jacquot S, Hanauer A and Allis CD (1999) Requirement of Rsk-2 for epidermal growth factor-activated phosphorylation of histone H3. *Science (Wash DC)* **285:**886–891.
Sauve DM, Anderson HJ, Ray JM, James WM and Roberge M (1999) Phosphorylation-induced rearrangement of the histone H3 NH2-terminal domain during mitotic chromosome condensation. *J Cell Biol* **145:**225–235.
Shen X, Yu L, Weir JW and Gorovsky MA (1995) Linker histones are not essential and affect chromatin condensation in vivo. *Cell* **82:**47–56.
Shevchenko A, Wilm M, Vorm O and Mann M (1996) Mass spectrometric sequencing of proteins from silver-stained polyacrylamide gels. *Anal Chem* **68:**850–858.
Stennicke HR and Salvesen GS (1997) Biochemical characteristics of caspases-3, -6, -7, and -8. *J Biol Chem* **272:**25719–25723.
Thomson S, Clayton AL, Hazzalin CA, Rose S, Barratt MJ and Mahadevan LC (1999) The nucleosomal response associated with immediate-early gene induction is mediated via alternative MAP kinase cascades: MSK1 as a potential histone H3/HMG-14 kinase. *EMBO J* **18:**4779–4793.
Tikoo K and Ali Z (1997) Structure of active chromatin: covalent modifications of histones in active and inactive genes of control and hypothyroid rat liver. *Biochem J* **322:**281–287.
Tikoo K, Gupta S, Hamid QA, Shah V, Chatterjee B and Ali Z (1997) Structure of active chromatin: isolation and characterization of transcriptionally active chromatin from rat liver. *Biochem J* **322:**273–279.
Trump BE, Berezesky IK, Chang SH and Phelps PC (1997) The pathways of cell death: oncosis, apoptosis, and necrosis. *Toxicol Pathol* **25:**82–88.
Wei Y, Yu L, Bowen J, Gorovsky MA and Allis CD (1999) Phosphorylation of histone H3 is required for proper chromosome condensation and segregation. *Cell* **97:**99–109.
Walisser JA and Thies RL (1999) Poly(ADP-ribose) polymerase inhibition in oxidant-stressed endothelial cells prevents oncosis and permits caspase activation and apoptosis. *Exp Cell Res* **251:**401–413.
Wolffe A (1995) *Chromatin Structure and Function*, Academic Press, New York.
Zingarelli B, Salzman AL and Szabo C (1998) Genetic disruption of poly (ADP-ribose) synthetase inhibits the expression of P-selectin and intercellular adhesion molecule-1 in myocardial ischemia/reperfusion injury. *Circ Res* **83:**85–94.

Address correspondence to: Terrence J. Monks, Ph.D., Center for Molecular and Cellular Toxicology, Division of Pharmacology & Toxicology, College of Pharmacy, University of Texas at Austin, Austin TX, 78712-1074. E-mail: scouser@mail.utexas.edu